

Ab-initio study of the segregation and electronic properties of neutral and charged B and P dopants in Si and Si/SiO₂ nanowires

Bob Schoeters,^{1,2,a)} Ortwin Leenaerts,^{1,b)} Geoffrey Pourtois,^{2,3,c)} and Bart Partoens^{1,d)}

¹Department of Physics, University of Antwerp, Groenenborgerlaan 171, B-2020 Antwerp, Belgium

²IMEC, Kapeldreef 75, B-3001 Leuven, Belgium

³Department of Chemistry, University of Antwerp, Universiteitsplein 1, B-2610 Wilrijk-Antwerp, Belgium

(Received 16 February 2015; accepted 23 August 2015; published online 9 September 2015)

We perform first-principles calculations to investigate the preferred positions of B and P dopants, both neutral and in their preferred charge state, in Si and Si/SiO₂ core-shell nanowires (NWs). In order to understand the observed trends in the formation energy, we isolate the different effects that determine these formation energies. By making the distinction between the unrelaxed and the relaxed formation energy, we separate the impact of the relaxation from that of the chemical environment. The unrelaxed formation energies are determined by three effects: (i) the effect of strain caused by size mismatch between the dopant and the host atoms, (ii) the local position of the band edges, and (iii) a screening effect. In the case of the SiNW (Si/SiO₂ NW), these effects result in an increase of the formation energy away from the center (interface). The effect of relaxation depends on the relative size mismatch between the dopant and host atoms. A large size mismatch causes substantial relaxation that reduces the formation energy considerably, with the relaxation being more pronounced towards the edge of the wires. These effects explain the surface segregation of the B dopants in a SiNW, since the atomic relaxation induces a continuous drop of the formation energy towards the edge. However, for the P dopants, the formation energy starts to rise when moving from the center but drops to a minimum just next to the surface, indicating a different type of behavior. It also explains that the preferential location for B dopants in Si/SiO₂ core-shell NWs is inside the oxide shell just next to the interface, whereas the P dopants prefer the positions next to the interface inside the Si core, which is in agreement with recent experiments. These preferred locations have an important impact on the electronic properties of these core-shell NWs. Our simulations indicate the possibility of hole gas formation when B segregates into the oxide shell.
 © 2015 AIP Publishing LLC. [<http://dx.doi.org/10.1063/1.4930048>]

I. INTRODUCTION

The behavior of dopant impurities in monocrystalline semiconductor nanostructures has been studied intensively in the last decade because of their role in controlling electronic properties. A few examples for silicon nanowires (SiNWs) can be found in Refs. 1–3 or in the references included in the following review.⁴ Dopants are less effective in creating free carriers in these nanostructures than in bulk due to confinement effects⁵ that lead to an increase of the ionization energies. The impurity atoms tend to segregate towards the surface which results in a highly non-uniform dopant distribution.⁶ Furthermore, the presence of dopants at the surface can induce changes into the scattering process occurring during transport. A thorough understanding of the dopant properties is therefore crucial to use such nanostructures as building blocks of opto-electronic devices.

The nanostructures under study in this paper are thin SiNWs. A common way to obtain such nanowires consists in starting from thicker wires, with a diameter of, e.g., 40 nm, and performing a thermal oxidation process to reduce the

diameter.⁷ This results in a narrow Si core surrounded by a thicker amorphous SiO₂ shell. Depending on the envisioned application, it is possible to either chemically etch away the oxide afterwards or to keep the obtained core-shell structure in order to exploit the beneficial dielectric properties of SiO₂. The properties of these Si/SiO₂ core-shell nanowires differ from commonly studied H passivated SiNWs: for instance, the band gap of the SiNWs is affected by the thickness of the surrounding SiO₂ layer and depends on the relative orientation of the SiNW.⁸ This results from the stress generated at the Si/SiO₂ interface induced by their lattice mismatch.^{9,10} A recent experimental study of SiNWs indicated that B and P impurities segregate towards the Si/SiO₂ interface during thermal oxidation. It was observed that P remains on the Si side while B moves inside the SiO₂ shell.¹¹ This differs from the trends reported for unoxidized SiNWs, where the edge positions are the preferred ones.³ *Ab initio* calculations of the formation energies of B and P in Si/SiO₂ indicate that the favored positions of these dopants are located close to the Si/SiO₂ interface.¹² These simulations suggest that substitutional B and P prefer positions around the interface, but just inside the Si core.

The origin of the segregation process of neutral dopants in H-passivated Si nanoclusters (quantum dots) has recently been discussed. Ma and Wei argued that two effects

^{a)}Electronic address: bob.schoeters@uantwerpen.be

^{b)}Electronic address: ortwin.leenaerts@uantwerpen.be

^{c)}Electronic address: Geoffrey.Pourtois@imec.be

^{d)}Electronic address: bart.partoens@uantwerpen.be

determine the preferential positions of the dopants:¹³ their chemical environment and their structural relaxation. The chemical environment favors the center of the dots, while the structural relaxation favors the edge as the most preferable position for dopants. The relative importance of the two effects depends on the size of the dopant atoms. When the size mismatch is large, as in the case of the B atoms, the relaxation effect is dominant. However, for similarly sized atoms such as the P ones, the chemical effect dominates. For H-passivated thin SiNW's, *ab initio* calculations indicate that B and P impurities both tend to segregate towards the surface of the SiNWs,³ suggesting that for thin SiNWs, the relaxation contribution is dominant.

For bulk Si, doping with either a B or P impurity atom results in the creation of an acceptor level close to the valence band maximum (VBM) (45 meV) or in a donor one close to the conduction band minimum (CBM) (44 meV), respectively. For thin nanowires, these levels lie deeper in the band gap due to quantum and dielectric confinement. According to tight-binding calculations, the doping with B or P in a 2 nm SiNW results into ionization energies of, respectively, 450 meV or 400 meV.⁵ Whereas an *ab initio* study using hybrid functionals predict ionization energies of 210 meV and 310 meV for, respectively, a [110] and a [111]-oriented 2 nm SiNW.¹⁴ In core-shell structures, it might be possible to circumvent this problem of large ionization energies, as in these systems, the effect of the dopants on the electronic structure depends on both the position of the dopant (core or shell) and on the band offset present between the core and the shell. An example of the effect of doping in core-shell nanowires has already been studied using first-principle calculations for core-shell Si/Ge nanowires.¹⁵ This study was motivated by the experimental observation of a 1D hole gas at the VBM in core-shell Si/Ge nanowires.¹⁶ The calculations indicate that these hole gases can be created by selectively doping a specific core-shell structure. If a B impurity is placed in the shell of a Ge(core)/Si(shell) nanowire, an acceptor level is induced above the valence bands of Si. However, due to the type-II band offset between Si and Ge, this level does not lie within the band gap of the nanowire, since the valence band edge states are composed of Ge bands. An electron from the VBM is transferred deeper into the valence band to fill up the created acceptor level, leaving a free hole at the VBM. Completely analogous, a P dopant inside the Ge core results in a free electron at the CBM. These kinds of free carriers can be very beneficial for applications since no thermal activation is required. Analogously, *ab initio* calculations predict the formation of hole gases in InAs/InP core-shell nanowires when doped with Zn inside the InP shell.¹⁷ However, Si and SiO₂ show a type-I band offset and thus, different electronic properties can be expected due to doping.

In this paper, we investigate the substitutional doping of H-passivated Si and Si/SiO₂ nanowires with B and P dopants. We determine the impact of the chemical environment and of the structural relaxation on the segregation process by building further on the ideas and results presented first by Ma *et al.* for dopants in Si clusters. However, we also focus on the dopants in their preferred charge state and show that

the mechanism that determines the preferential position differs for neutral and charged dopants. The relaxation effect is also quantified in relation to the size of the impurities. For the Si/SiO₂ nanowires, we also investigate the influence of the position of the dopants in the structure on the electronic properties. This paper is further organized as follows. First, our methodology is presented. Then, we discuss the case of doping of H-passivated SiNWs. This section is an extension of an earlier work³ that we reinterpret on the basis of both the chemical environment and the structural relaxation. We investigate the impact of the dopant size by using C and Ge and analyze the chemical effect through neutral and ionic B and P dopants. Finally, we discuss the localization of the B and P impurity dopants in Si/SiO₂ nanowires and their impact on the electronic properties.

II. COMPUTATIONAL DETAILS

Ab initio Density Functional Theory calculations, as implemented in the OpenMx code,^{18–20} were performed on Si and Si/SiO₂ nanowires using the Generalized Gradient Approximation (GGA) developed by Perdew, Burke, and Ernzerhof.²¹ We used a double-valence plus single-polarization orbital basis set. For a single nanowire unit cell, a Monkhorst-Pack k-point grid²² of $1 \times 1 \times 6$ was used. Most of the defect calculations were performed using a supercell of three unit cells along the periodic direction of the nanowire axis. Here, we use an equivalent $1 \times 1 \times 2$ k-point grid. To minimize the interaction between the different periodic images, a vacuum of at least 1 nm was used in the directions perpendicular to the axis of the wires. The accuracy of the numerical integrations and of the solving of the Poisson equation within OpenMx are defined using a grid fineness, which we fixed by using a cutoff energy of 150 Rydberg (2040 eV). All the structures discussed below are relaxed using the method developed by Baker²³ until the forces working on the atoms are smaller than 0.05 eV/Å. For the calculations of the electronic properties, i.e., band structure and density of states (DOS), we used a denser k-point grid of $1 \times 1 \times 10$.

In order to determine the energetically most stable locations of neutral B and P dopant in the nanowires, we substitute a Si atom by a B or P dopant and compute its associated formation energy as

$$E_f = E(\text{doped SiNW}) - E(\text{SiNW}) + \mu_{\text{Si}} - \mu_{\text{B/P}} \quad (1)$$

It is important to note that only the absolute value of the formation energy is changed by the choice of the chemical potentials, the differences between the different positions does not depend on this choice. Given the fact that we are only interested in the differences of the formation energies and to facilitate the comparison between the formation energies of different dopants and different charged states, we make the choice to put the unrelaxed formation energy of the dopants at position 1 equal to zero. Therefore, this represents a relative formation energy and not the absolute one.

Besides neutral formation energies we also look at the energies in the preferred charge states. Typically, to study charged defects, a uniform background charge is added, to

keep the supercell neutral. This approach is well defined for bulk systems. However, it is problematic for nanostructures where much of the supercell corresponds to vacuum, and as a consequence the total energy will depend on the size of this vacuum. Therefore, it is not straightforward to calculate formation energies of charged defects in nanostructures, although recently an elaborate correction scheme has been proposed.²⁴ This correction scheme changes the absolute value of the formation energy but not the trend between dopants at different positions inside the considered system, which means that energy differences between charged defects at different positions in the same nanowire, without corrections, are meaningful.

For the charged dopants, it is also important to note that in order to achieve a converged result for the total energy of the charged dopants a larger supercell than three unit cells is required as described in Ref. 25. However, the relative formation energies are converged within 0.01 eV.

III. RESULTS AND DISCUSSION

A. H-passivated Si nanowires

We start our study by investigating the substitutional doping in H-passivated Si nanowires. Our model system consists of a 2.2 nm [100]-oriented nanowire as shown in Fig. 1. We calculate the formation energies for nine inequivalent dopant positions, as depicted in the figure, which are numbered from (1) to (9) when moving from the center of the wire towards the surface. The last positions at the surface which are bonded to the hydrogen are not considered in this study. To understand the various influences of the impurities on the dopant formation energy, we try to isolate the different contributing effects of the substitutional atoms. Following the results of Ma and Wei¹³ for doping in Si nanoclusters, we distinguish the environmental (or chemical) and relaxation effects. The environmental effect is defined as the

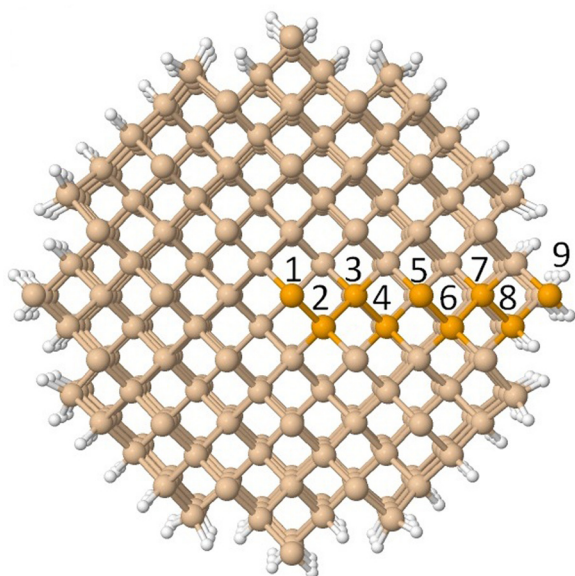


FIG. 1. Illustration of the supercell used to model the Si nanowire. The Si atoms are depicted in pale grey and H in white. The orange ones are the Si sites substituted by dopants.

changes in the properties of the wire that follow from substituting a silicon atom with a dopant one without allowing a relaxation of the structure. The formation energy for the unrelaxed and relaxed structures will be investigated for different types of dopants to analyze the various influences even further.

The bond lengths between the various Si atoms in an undoped wire are not constant. Due to relaxation effects, the average bond length slightly increases when going from the center of the wire to the surface, as shown in Fig. 2(a). Close to the surface, a sharp decrease in bond length is observed. The varying bond lengths can be expected to have some influence on the formation energy. Small atoms (as compared to Si) might prefer shorter bond lengths and consequently the center or the edge of the nanowire, while the opposite is true for large atoms. This size effect is nicely illustrated by using impurities that are chemically similar to Si but have different sizes. C and Ge atoms fulfill these requirements well because they possess an equal number of valence electrons and have covalent radii²⁶ that are, respectively, smaller (70 pm) and slightly larger (125 pm) than that of Si (110 pm). Therefore, C should fit better at positions with smaller bond lengths while the opposite is true for Ge. Upon substitution of C and Ge in the SiNW (without relaxation), this dependence of the formation energy on the average bond length size is clearly observed, as can be seen in Fig. 2(b). The effect is more pronounced for C because the size mismatch between C and Si is larger than that between Ge and Si.

Another, more pronounced, effect induced by the size mismatch between the dopant and host atoms is observed when including the relaxation in the system. The formation energies before and after relaxation are shown in Fig. 2. The mismatch between Si and Ge is small, so only a weak relaxation occurs in that case. However, due to the large size mismatch in the atomic radius between C and Si, a more pronounced relaxation is possible, which leads to a substantial decrease in the formation energy. A second observation that can be made is that the relaxation at the edge is larger than at the center.^{3,13} In other words, the relaxation effect favors the edge over the center of the nanowire.

Interestingly, the observed trend in the formation energy can again be understood in terms of the average bond lengths of the dopants with the surrounding atoms. The average bond lengths after relaxation of, respectively, C and Ge are depicted in Figs. 2(c)–2(e). In the case of the C dopants the average bond lengths decrease when moving towards the edge, which is clearly translated in the formation energy of these dopants since the C atoms prefer the positions with the smaller average bond lengths. The reason for these smaller bond lengths when moving towards the edge is that the relaxation becomes less restricted when moving away from the center. In the case of the Ge dopants the situation is somewhat reversed. These dopants prefer the positions with the largest average bond length. The relaxation effect is again larger towards the edge and thus the average bond length increases when moving away from the center lowering the formation energy.

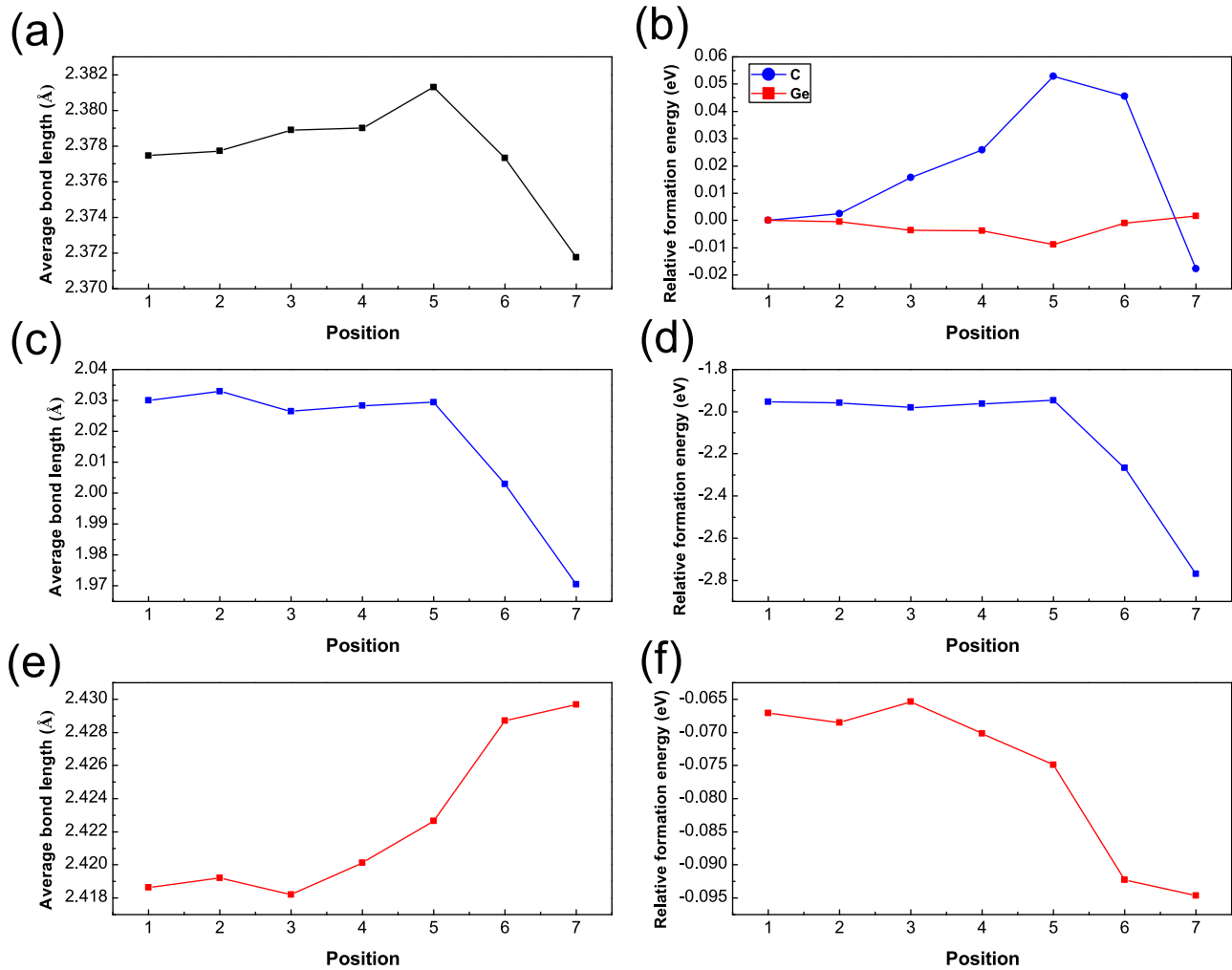


FIG. 2. (a) Average bond length of the Si atoms at different atomic positions going from 1 to 7 with the surrounding Si atoms. (b) Unrelaxed relative formation energy of C (blue) and Ge (red) in the SiNW's. (c)–(e) The average bond lengths, after relaxation, of, respectively, C and Ge at the different atomic positions. (d)–(f) The relaxed relative formation energy of, respectively, C and Ge.

Next, we study the substitutional doping with B and P atoms in the SiNW. We consider both neutral and charged dopants and show the unrelaxed formation energy at the different substitution sites in Fig. 3. It is seen that the formation energy increases towards the edge of the wire, regardless of the type and charge state of the dopants, although the neutral dopants exhibit a more pronounced dependence on the radial distance.

A similar trend for the neutral B and P dopants in small Si nanoclusters has been explained in the literature¹³ as follows: confinement tends to shift both valence and conduction bands away from the bulk gap when approaching the edge of the system. Therefore, acceptor levels created near the top of the valence band (as in the case of B impurities) will be lower in energy near the surface. Because it costs more energy to have a missing electron at a lower energy level,

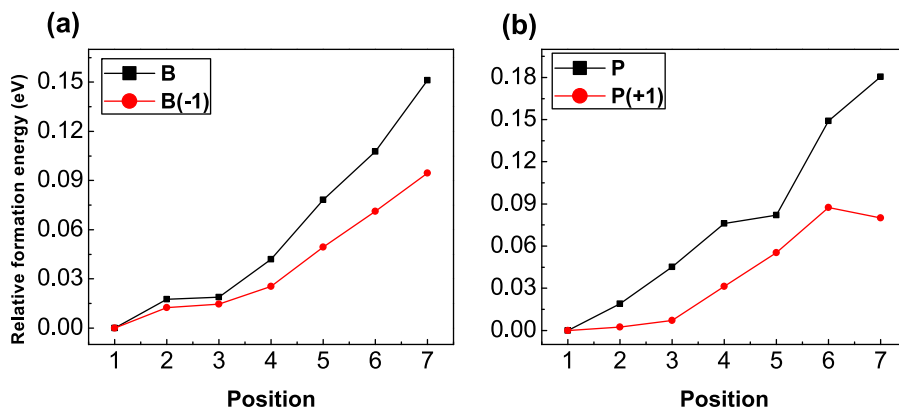


FIG. 3. Neutral (black) and charged (red) unrelaxed relative formation energies of (a) B and (b) P in the SiNW.

the formation energy for B dopants is larger towards the edge. Similarly, donor states near the bottom of the conduction band (as in the case of P impurities) will be higher in energy near the surface. Consequently, an extra electron in this state will have higher energy near the edge and the formation energy will be larger there. If this hypothesis is correct, the formation energy should not increase towards the edge if we do not have holes in the acceptor level and electrons in the donor level, as in the case of B^- and P^+ dopants, respectively. However, our results of the formation energies of the charged impurities show that the trends still persists, although less pronounced. Therefore, this explanation is incomplete.

In order to explain these observations in more depth, it is helpful to split the doping process into two parts: (i) the dopant gives rise to a screened Coulomb potential because of its additional core charge of ± 1 , and (ii) an extra electron or hole is introduced in the system due to the different number of valence electrons. The first part can be isolated by the examination of charged dopants. Such ionic doping leaves the number of electrons unchanged as compared to the undoped SiNW and only adds a negative/positive unit of charge on a particular nucleus. Therefore, only an impact of this extra potential is observed. The SiNW can be regarded as a neutral background to which the extra core potential is added. Independent of the sign of the additional potential, it will be better screened in the middle of the wire than closer to the edge because the dielectric constant of Si is larger than that of vacuum. Therefore, the formation energy is expected to increase towards the edge for both B^- and P^+ dopants.

In the case of neutral B and P dopants, the effect of the extra hole or electron is included. From the spatial position of the VBM and CBM in Fig. 4(a) and the local position of the band edges at the various atomic sites, as depicted in Fig. 4(b), it is seen that extra electrons or holes tend to occupy the middle of the wire in pure SiNWs. The formation energy will be lower if the interaction between this charge carrier and the screened Coulomb potential is strongest, i.e., in the middle of the wire. In other words, the trend of the charged dopants will be enhanced by removing the charge from the system.

The relaxation effect is opposite to the chemical one discussed above and the two contributions will compete with each other. The effect that will dominate depends on the type of atom and on its charge. In the case of B, the large size

mismatch is such that the relaxation dominates. This explains why the formation energy of B drops when moving towards the surface, reaching a minimum just next to the edge (Fig. 5(a)). This suggests that the mechanism driving the formation energy of impurity dopants in H-passivated Si nanoclusters,¹³ which we discussed in the Introduction, can also be extended to the case of H-passivated nanowires.

For P dopants, the chemical and relaxation effects are more balanced. The chemical trend of the neutral P dopants is strong enough to resist the relaxation contribution and leads to a favorable position at the center. However, a local minimum close to the edge (at position 7) is created by relaxing the structure. For P^+ atoms, the chemical impact is smaller because the confinement energy of the electron is absent. The local minimum that was observed for the neutral P atom becomes a global minimum, so that the dopant is most likely to be located near the edge.

Note that the same trends can also be observed in thinner H-passivated SiNW (with radius 1.6 nm) in Fig. 3 of Ref. 3, although in that case, the minimum in the formation energy of the P dopant at the edge of the wire is the global minimum.

B. Si/SiO₂ core-shell nanowire

To determine the behavior of B and P doping in core-shell Si/SiO₂ nanowires, we consider a simple model consisting of an ~ 1.1 nm [100]-oriented crystalline Si core surrounded by a crystalline SiO₂ layer, resulting in a total diameter of 2.2 nm [Fig. 6(a)]. This model is built from a pure SiNW by expanding the Si-Si bonds and inserting oxygen atoms in between (starting from a nanowire radius of 1.1 nm) and fully relaxing the structure afterwards. Although more complicated models are described in the literature,^{8,10,12,27} this simple one is adequate to capture the experimentally observed behavior. The band offset between the Si core and the SiO₂ shell in the nanowire can be estimated from the projected DOS (PDOS), which is shown in Fig. 7. Note that the band gap computed at the GGA level is 1.4 eV, where the band gap for the H passivated SiNWs with the same diameter is 2.5 eV. The origin of the band gap reduction is related to the stress induced by the SiO₂ layer. The computed band gap of 6.4 eV for SiO₂ is larger than the one expected for bulk SiO₂ (5.7 eV) using the GGA approximation,²⁸ which is a consequence of the quantum confinement.

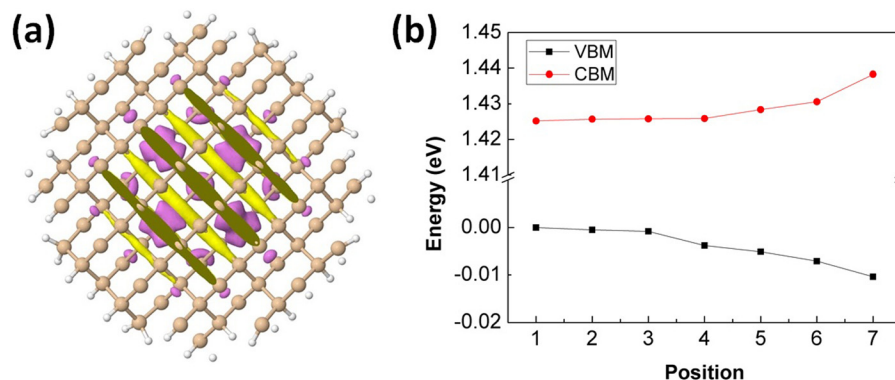


FIG. 4. (a) Partial charge densities of the VBM (yellow) and CBM (violet) plotted on the SiNW. (b) Local position of the VBM and CBM obtained by looking at the PDOS at the different positions.

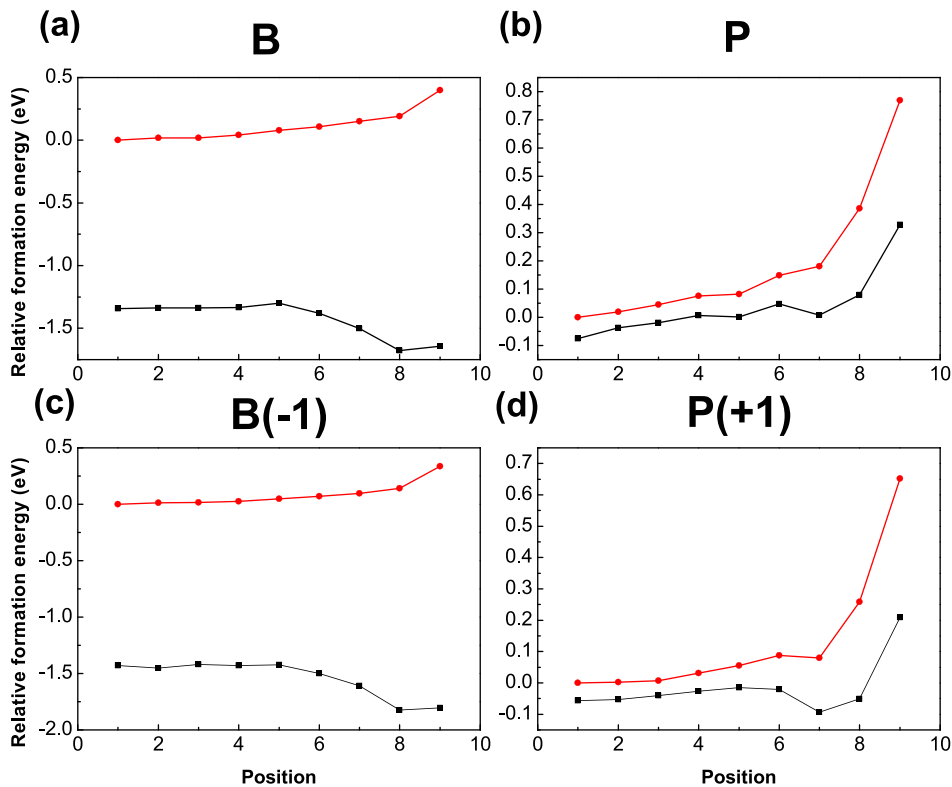


FIG. 5. Relative formation energies, before (red) and after atomic relaxation (black), of the H passivated SiNW. (a) neutral B, (b) neutral P, (c) B⁻ and (d) P⁺.

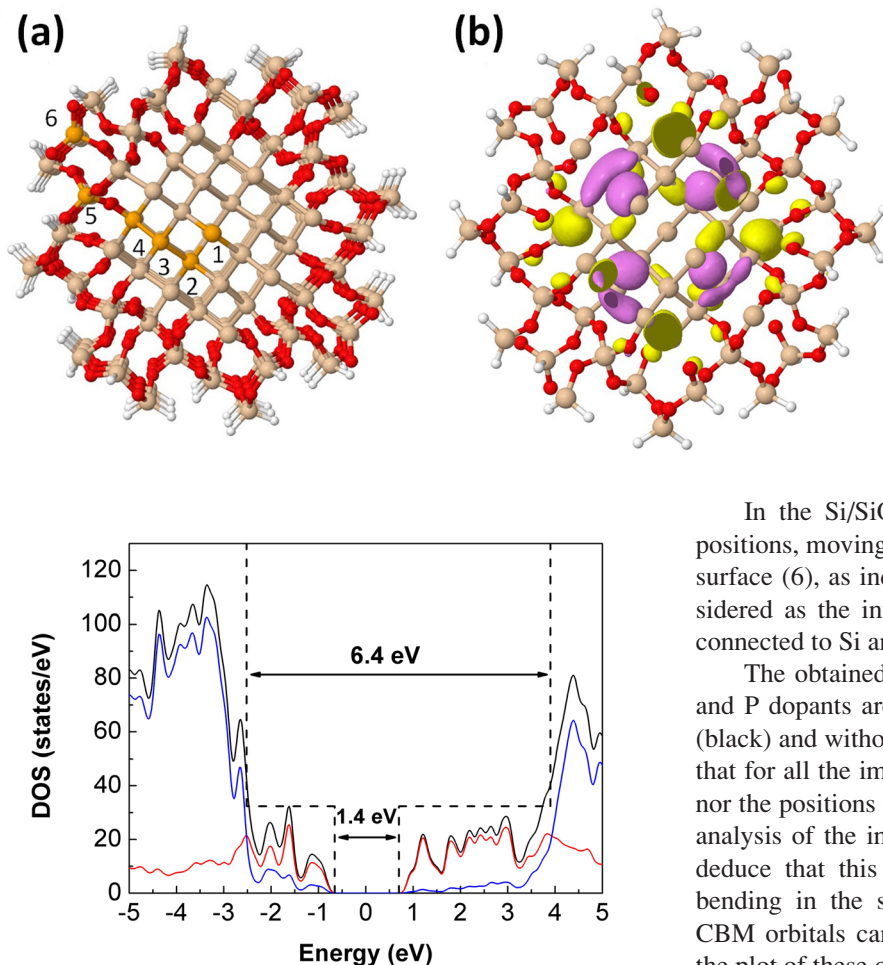
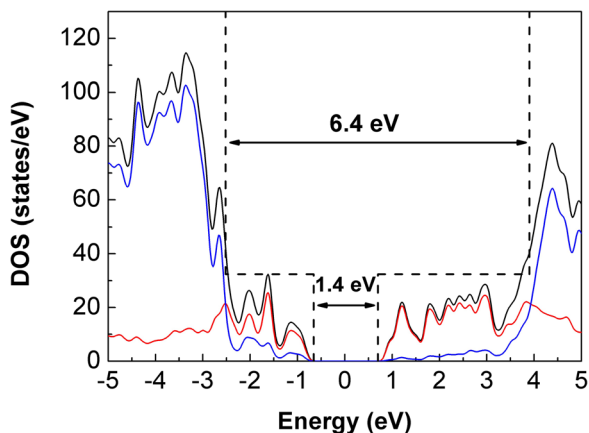


FIG. 6. (a) Illustration of the supercell used to model the Si/SiO₂ NW. The Si atoms are depicted in pale grey, O in red and H in white. The orange ones are the Si sites substituted by dopants. (b) Partial charge densities of the VBM (yellow) and CBM (violet) plotted on the Si/SiO₂ NW.

FIG. 7. DOS of the Si/SiO₂ NW (black) and the projected density of states of the Si core (red) and the SiO₂ shell (blue).



In the Si/SiO₂ nanowire, we look at six inequivalent positions, moving from the center (1) of the wire towards the surface (6), as indicated in Fig. 6(a). Position 4 can be considered as the interface between Si and SiO₂ because it is connected to Si and O atoms.

The obtained formation energies of neutral and ionic B and P dopants are summarized in Fig. 8 for structures with (black) and without (red) atomic relaxation. It can be noticed that for all the impurities, neither the positions in the center, nor the positions close to the surface are favorable. From the analysis of the impurity doping in the Si nanowire, we can deduce that this should be related to the electronic band bending in the structure. The positions of the VBM and CBM orbitals can be used to localize these extrema. From the plot of these orbitals in Fig. 6(b), we can see that they are situated near the interface, in contrast to those of the H-passivated SiNW, which are located at the center of the wire

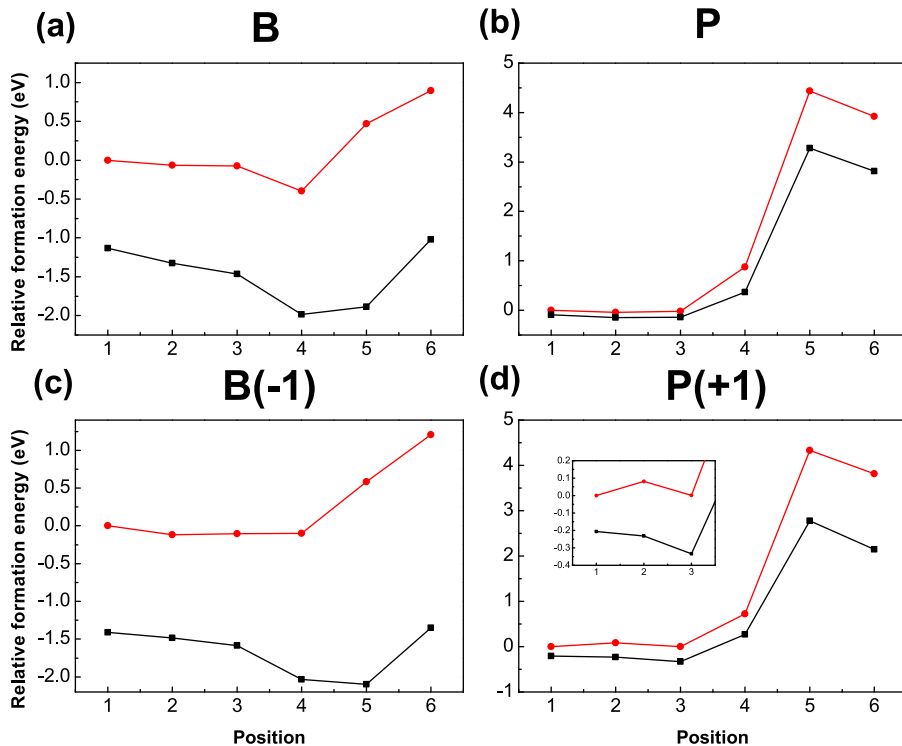


FIG. 8. Relative formation energies, before (red) and after relaxation (black), of the SiSiO₂ NW. (a) Neutral B, (b) neutral P, (c) B⁻, and (d) P⁺.

(see Fig. 1). The origin of this localization at the interface might be related to the interfacial strain that causes the band gap to decrease.

The localization effect also appears to be stronger for the VBM than for the CBM which is still located in the Si core. This can be explained by an upward band bending near the interface due to a charge depletion at the edge of the core. This charge depletion results from the larger electronegativity of O as compared to Si atoms, as evidenced by the Mulliken charges of the Si atoms depicted in Fig. 9. In the valence band, the strain-induced reduction of the band gap and the upward band bending both ensure a localization of the VBM at the interface. In the conduction band, however, the effect of band bending is opposite to that of the gap reduction, resulting in a CBM that remains in the Si core but is shifted towards the edge.

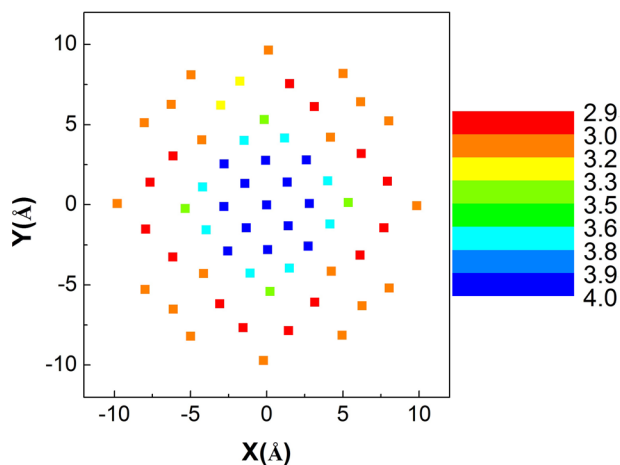


FIG. 9. Mulliken charge of the Si atoms in the Si/SiO₂ NW.

We will now discuss the various dopants in more detail, starting with the neutral B and P. Without relaxation, the B impurity prefers to occupy the position at the interface between Si and SiO₂, which is consistent with the position of the wavefunction of the VBM (indicated in yellow in Fig. 6(b)). For P in the unrelaxed configuration, the differences between locations 1 to 3 within the Si core are relatively small (less than 0.1 eV), with position 2 having the lowest formation energy. This is also consistent with the localization of the CBM (indicated in purple in Fig. 6(b)). The localization of B and P inside SiO₂ is not energetically favored based on the unrelaxed energies. The impact of the atomic relaxation is minimal on the formation energies of P, as is expected from the small atomic radius mismatch between P and Si. As expected from the size mismatch, the relaxation for the B atoms results in a large downshift of the formation energies by about 1 eV. The impact of the atomic reorganization is the strongest at the surface and around the interface where the system has less constraints. Position 4 at the Si/SiO₂ interface remains the most stable one but the difference with respect to position 5 (just inside the SiO₂ shell) is small (≈ 0.1 eV).

Let us now consider the dopants in their preferred charge states, before and after relaxation. The energy of the B⁻ and P⁺ dopants at the different positions are shown in Figs. 8(c) and 8(d), respectively. Without relaxation, the energetically preferred position for B⁻ is position 4 at the interface, but the difference with the positions inside the Si core is smaller than in the neutral case. This is consistent with the less pronounced trends in formation energy for the ions in the SiNW discussed above. The difference is enhanced by the relaxation process, but the largest relaxation occurs inside the SiO₂. This makes of position 5, close to the interface but just inside the SiO₂, the preferred location. For P⁺

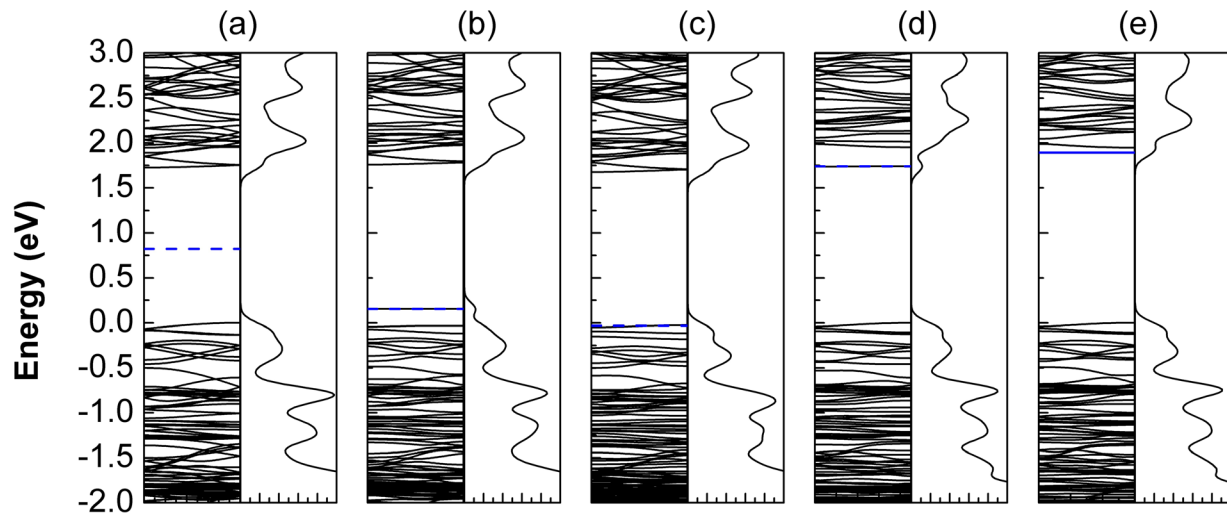


FIG. 10. Band structure and DOS of (a) Undoped Si/SiO₂ nanowire, (b) B doped at positions 4 inside the core, (c) B doped at position 5 inside the shell, (d) P doped at positions 4 inside the core, (e) P doped at position 5 inside the shell. The blue dashed line corresponds to the calculated Fermi level. The band structures are aligned relative to the vacuum level and the zero of the energy is taken to be the VBM of the undoped wire.

dopants, the energetically preferred position without relaxation is position 3, i.e., in the Si core but close to the interface. There is also a local minimum at the center of the Si core that disappears after relaxation.

In conclusion, the formation energies of the charged B and P dopants suggest that B⁻ prefers being located just inside the SiO₂ near the interface, while P⁺ prefers occupying the positions near the interface inside the Si core. Both are in agreement with the experimental results reported in Ref. 11. Note that for the case of B dopants, our results differ from those obtained by Kim *et al.*¹² In that work, it was found that B atoms prefer to be positioned near the interface but inside the Si core. The origin of this disagreement is probably the larger average bond lengths at the interface in this work, resulting from the specific construction of the Si/SiO₂ nanowire. The model of Kim *et al.* consists of a perfect Si core that is fitted in an amorphous SiO₂ shell. This leads to larger average bond lengths that are unfavorable for B atoms, as we demonstrated above. Real Si/SiO₂ core/shell nanowires are obtained by oxidizing Si wires and are (in this respect) closer to our model.

C. Impact on electronic properties

To investigate the impact of B and P doping on the electronic properties, we report their effect on the band structure at two different positions in the wire; at position 4, just at the Si/SiO₂ interface and at position 5, inside the SiO₂ shell. In Fig. 10, the band structure and the DOS of both the undoped and the doped Si/SiO₂ nanowire is depicted. First, we discuss the impact of doping at position 4, for which the same behavior as in pristine SiNWs is expected. Figs. 10(b) and 10(d) show that both B and P doping inside the Si core result in the creation of an acceptor or donor level inside the band gap, corresponding to the flat bands associated with ionization energies of, respectively, 192 meV and 214 meV. It is important to note that the states that are induced by B/P doping inside the band gap mainly have Si character, as illustrated by the PDOS of the P doped NW, Fig. 11, and can hence be

considered as hydrogenic impurities instead of localized atomic impurity levels. Other (minor) effects are also visible in the band structures, such as the lifting of the degeneracy of the highest valence band at Γ or the lowest one at X . However, these effects are attributed to a symmetry breaking induced by the relaxation around the impurity atom. Since a concentration of $\approx 10^{20} \text{cm}^{-3}$, i.e., one impurity dopant in three unit cells represents a very high density, we checked the consistency of the obtained results using six times the smallest unit cell (not shown). The obtained position of the levels inside the band gap is the same as for three unit cells indicating that the model captures the essence of the change in electronic properties driven by the impurity doping.

However, if we place the dopant inside the SiO₂ shell positions, a different behavior is observed. Figs. 10(c) and 10(e) show the corresponding band structures. For both the B and P doping inside SiO₂, no acceptor/donor levels are induced inside the band gap. Interestingly, the Fermi level is located, respectively, at the VBM or CBM. We attribute this effect to the one reported for the SiGe nanowires in Ref. 15.

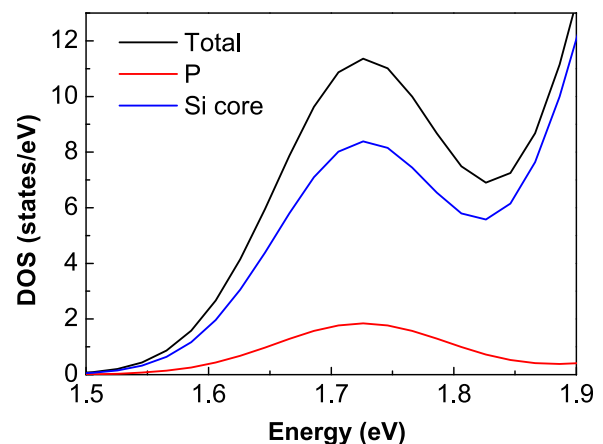


FIG. 11. Partial DOS of the defect level induced inside the band gap by the P dopant. The black line corresponds to the total DOS, red to the PDOS of the P and blue to the Si core atoms.

Indeed, for B (P) doping the acceptor (donor) level is induced above the valence bands (below the conduction bands) of SiO₂, but due to the type-I band offset these states are still located below (above) the Si states at the band edges. Therefore, no state is observed inside the band gap but a free hole (electron) becomes available at the VBM (CBM). This implies that doping inside the SiO₂ shell could induce electron or hole gases at the band edges. Since the formation energies indicate that P prefers to stay in the Si core, we do not expect a large amount of free electrons to become available at the CBM. However, B dopants are more likely to segregate into the shell. The creation of hole gases is hence more probable. While these hole gases have been observed experimentally for SiGe nanowires, we are not aware of this having been reported for Si/SiO₂ nanowires.

IV. CONCLUSIONS

In this paper, we investigated the formation energies of substitutional B and P dopants in H-passivated Si and core-shell Si/SiO₂ nanowires using first-principles simulations. Several important properties of the dopants and the wires that influence the formation energies have been isolated. First, we used C and Ge dopants to illustrate the influence of the atomic size on the formation energy with and without atomic relaxation. A large size mismatch was shown to cause substantial relaxation effects that reduce the formation energy considerably. This effect was shown to be the strongest at the edge.

By considering ionic B and P dopants, we were able to distinguish the chemical effects that influence the formation energy: (i) The local position of the VBM (CBM) which decreases (increases) in energy towards the edge of the H-passivated nanowire and increases (decreases) towards the interface in Si/SiO₂ core-shell nanowires. (ii) The screening effect which is strongest in the center of the NW's.

We used the effect of the chemical environment and of the structural relaxation to explain the preferred locations of B and P in SiNWs. The lowest formation energy for the neutral B dopants is at the edge of the wire due to the large atomic relaxation. For the B⁻, the trend of the formation energy remains the same as for the neutral one. However, for the P dopants, the trend is very different. There is only a little relaxation resulting in a minimum for the energy in the center of the nanowire. The charged P⁺ dopants have a global minimum close to the edge, whereas this was only a local minimum for the neutral ones. In the Si/SiO₂ nanowires the dopants prefer positions close to the interface. The neutral B dopants prefer the position at the interface, connected to both the Si core and the oxide shell, close to the physical location of the VBM. Note that the difference with the position inside the oxide shell is small. When an extra electron is included in the system the localization of the VBM will no longer impact the formation energy, therefore the position just inside the oxide shell becomes the preferred one. The

formation energies of the neutral and the charged P appear to be very similar. In both cases, the energies are lowest in the Si core with only a small difference in energy between the different positions. However, for the P⁺ dopants, the position at the edge of the Si core but not connected with the oxide is the preferred position. Both the preferred locations of the charged dopants are in agreement with the experimentally observed segregation behaviour of these dopants during thermal oxidation.

Our study of the electronic properties also revealed that doping inside the Si core results in defect levels which lie deep in the band gap, whereas doping inside the SiO₂ shell results in the creation of a free hole (electron) at the VBM (CBM). This is of interest since these carriers do not require any thermal activation.

ACKNOWLEDGMENTS

This work was carried out using the Turing HPC infrastructure at the CalcUA core facility of the Universiteit Antwerpen, a division of the Flemish Supercomputer Center VSC, funded by the Hercules Foundation, the Flemish government and the Universiteit Antwerpen.

- ¹N. Fukata, *Adv. Mater.* **21**, 2829 (2009).
- ²Y. M. Niquet, L. Genovese, C. Delerue, and T. Deutsch, *Phys. Rev. B* **81**, 161301 (2010).
- ³H. Peelaers, B. Partoens, and F. M. Peeters, *Nano Lett.* **6**, 2781 (2006).
- ⁴R. Rurali, *Rev. Mod. Phys.* **82**, 427 (2010).
- ⁵M. Diarra, Y.-M. Niquet, C. Delerue, and G. Allan, *Phys. Rev. B* **75**, 045301 (2007).
- ⁶M. V. Fernández-Serra, C. Adessi, and X. Blase, *Phys. Rev. Lett.* **96**, 166805 (2006).
- ⁷H. I. Liu, D. K. Biegelsen, F. A. Ponce, N. M. Johnson, and R. F. W. Pease, *Appl. Phys. Lett.* **64**, 1383 (1994).
- ⁸R. J. Bondi, S. Lee, and G. S. Hwang, *ACS Nano* **5**, 1713 (2011).
- ⁹K.-H. Hong, J. Kim, S.-H. Lee, and J. K. Shin, *Nano Lett.* **8**, 1335 (2008).
- ¹⁰U. Khalilov, G. Pourtois, A. Bogaerts, A. C. T. van Duin, and E. C. Neyts, *Nanoscale* **5**, 719 (2013).
- ¹¹N. Fukata, S. Ishida, S. Yokono, R. Takiguchi, J. Chen, T. Sekiguchi, and K. Murakami, *Nano Lett.* **11**, 651 (2011).
- ¹²S. Kim, J.-S. Park, and K. J. Chang, *Nano Lett.* **12**, 5068 (2012).
- ¹³J. Ma and S.-H. Wei, *Phys. Rev. B* **87**, 115318 (2013).
- ¹⁴R. Rurali, B. Aradi, Th. Frauenheim, and A. Gali, *Phys. Rev. B* **76**, 113303 (2007).
- ¹⁵M. Amato, S. Ossicini, and R. Rurali, *Nano Lett.* **11**, 594 (2011).
- ¹⁶W. Lu, J. Xiang, B. P. Timko, Y. Wu, and C. M. Lieber, *Proc. Natl. Acad. Sci. U.S.A.* **102**, 10046 (2005).
- ¹⁷Q. Jiang, Z. Wen, and Q. Jiang, *Solid State Commun.* **152**, 2120 (2012).
- ¹⁸T. Ozaki, *Phys. Rev. B* **67**, 155108 (2003).
- ¹⁹T. Ozaki and H. Kino, *Phys. Rev. B* **69**, 195113 (2004).
- ²⁰T. Ozaki and H. Kino, *Phys. Rev. B* **72**, 045121 (2005).
- ²¹J. P. Perdew, K. Burke, and M. Ernzerhof, *Phys. Rev. Lett.* **77**, 3865 (1996).
- ²²H. J. Monkhorst and J. D. Pack, *Phys. Rev. B* **13**, 5188 (1976).
- ²³J. Baker, *J. Comput. Chem.* **7**, 385 (1986).
- ²⁴H.-P. Komsa and A. Pasquarello, *Phys. Rev. Lett.* **110**, 095505 (2013).
- ²⁵R. Rurali, M. Palummo, and X. Cartoixa, *Phys. Rev. B* **81**, 235304 (2010).
- ²⁶J. C. Slater, *J. Chem. Phys.* **41**, 3199 (1964).
- ²⁷U. Khalilov, G. Pourtois, A. C. T. V. Duin, and E. C. Neyts, *Chem. Mater.* **24**, 2141 (2012).
- ²⁸S. Park, B. Lee, S. H. Jeon, and S. Han, *Curr. Appl. Phys.* **11**, S337 (2011).